

# Facile and flexible fabrication of gapless microlens arrays using a femtosecond laser microfabrication and replication process

Hewei Liu<sup>a</sup>, Feng Chen<sup>\*a</sup>, Qing Yang<sup>b</sup>, Yang Hu<sup>a</sup>, Chao Shan<sup>a</sup>, Shengguan He<sup>a</sup>, Jinhai Si<sup>a</sup> and Xun Hou<sup>a</sup>

<sup>a</sup>Key Laboratory for Physical Electronics and Devices of the Ministry of Education & Shaanxi Key Lab of Information Photonic Technique, School of Electronics & information Engineering, Xi'an Jiaotong University, No. 28 Xianning West Road, Xi'an, 710049, P.R. China;

<sup>b</sup>State Key Laboratory for Manufacturing Systems Engineering, Xi'an Jiaotong University, No. 28 Xianning West Road, Xi'an, 710049, P. R. China

## ABSTRACT

We demonstrate a facile and flexible method to fabricate close-packed microlens arrays (MLAs). Glass molding templates with concave structures are produced by a femtosecond (fs)-laser point-by-point exposures followed by a chemical treatment, and convex MLAs are subsequently replicated on Poly(methyl methacrylate) [PMMA] using a hot embossing system. As an example, a microlens array (MLA) with 60- $\mu\text{m}$  rectangular-shaped spherical microlenses is fabricated. Optical performances of the MLAs, such as focusing and imaging properties are tested, and the results demonstrate the uniformity and smooth surfaces of the MLA. We also demonstrated that the shape and alignment of the arrays could be controlled by different parameters.

**Keywords:** Femtosecond laser, microfabrication, microlenses, hot embossing, glasses

## 1. INTRODUCTION

In the past decades, great efforts are made to develop a low-cost and efficient method to fabricate close-packed MLA. Up to now, the most widely used technique is a two-step process of a photolithograph followed a thermal reflow<sup>1-3</sup>. This method can produce large-area microlens arrays with spherical surfaces but sophisticated controlling processes are needed to fabricate close-packed MLAs. In addition, it is not convenient to control the shape of microlenses in high temperature. Gray-scale photolithograph can fabricate MLA in one step<sup>4</sup>; however the fabrication of mask is complex. Other techniques such as LIGA<sup>5</sup> and laser direct writing<sup>6</sup> present shape-controlled method to create spherical and aspherical microlenses, but suffers from expensive equipments and long processing times.

In this work, we propose a laser-based method to fabricate close-packed MLA on Poly(methyl methacrylate) [PMMA]. By femtosecond-laser point-by-point exposures followed by hydrofluoric acid solution etching process, concave spherical surfaces are self-formed on a silica glass chip. Serving the chip as mold template, the convex microlenses are replicated on a PMMA sheet by hot embossing process. This method is facile and efficient. As an example, an array with over 16,000 rectangular-shaped microlenses is fabricated within a few hours. An optical microscope (OM) [Eclipse LV100D, Nikon], and a scanning electronic microscope (SEM) [JSM-6390, JEOL] are utilized to observe the morphology of the microlenses. A three-dimensional (3D) laser confocal scanning microscope (LCM) [VK-9700, KEYENCE] is employed to measure the 3D profiles. A microscope system equipped with a computer-controlled 3D stage and a CCD camera is used to study the diffusion effect of the MLA.

## 2. EXPERIMENTAL

The close-packed MLA was fabricated on a PMMA sheet with a thickness of 1 mm; the procedures are schematically depicted in Fig. 1 (a). The glass mold of the MLA with rectangular shape was produced by a two-step process. The fabrication process can be monitored by the optical microscope and the OM images of the formation process are shown Figs. 1 (b)-(d). First, in situ laser exposures were carried out point-by-point on a polished silica glass chip (10 $\times$ 10 $\times$ 1 mm<sup>3</sup>) using a 30-fs and 800-nm laser pulses at a repetition of 1 kHz (the laser source is a Ti: sapphire pulsed laser

oscillator-amplifier system). The laser pulses with power of 2.5 mW (the laser power can be controlled by a variable attenuator) were focused by an objective lens ( $NA = 0.5$ ) and a fast mechanical shutter was used to control the exposure time. In the experiment, the exposure time was 500 ms. Because the energy density of the focused laser pulses we used in our experiments are much higher than the minimum energy density that results in the breakdown of the silica glass, which is so-called thresholds energy ( $\sim 0.44 \text{ J/cm}^2$ ), ablation-induced craters can easily observed on the sample surface, as shown in Fig. 1 (b). The diameter of the craters is about  $2 \mu\text{m}$ , and the interspacing between neighbor craters is  $60 \mu\text{m}$ . Second, the sample with craters was treated in 5% hydrofluoric (HF) acid solution assisted by an ultrasonic bath at  $23^\circ\text{C}$ . During this process, the chemical etch was significantly enhanced in the laser-induced craters because of the laser-induced modification of the surrounding materials, such as the heat-affected zones (HAZs)<sup>7</sup>, recrystallization<sup>8</sup> and formation of nano-cracks<sup>9</sup>, and the concave spherical surfaces began to form in the laser-exposure spots, as shown in Fig. 1 (c). The circular-shaped concave structures expand with the chemical etching process. When the neighbor ones contacted with each other, straight boundary lines are formed, eventually forming the rectangular patterns, as shown in Fig. 1 (d). The entire etching time for the formation of rectangular patterns was about 45 minutes. Finally, the fabricated mold was cleaned by the ultrasonic bath in acetone, alcohol and deionized water for 15 minutes, respectively, and dried in ambient air.

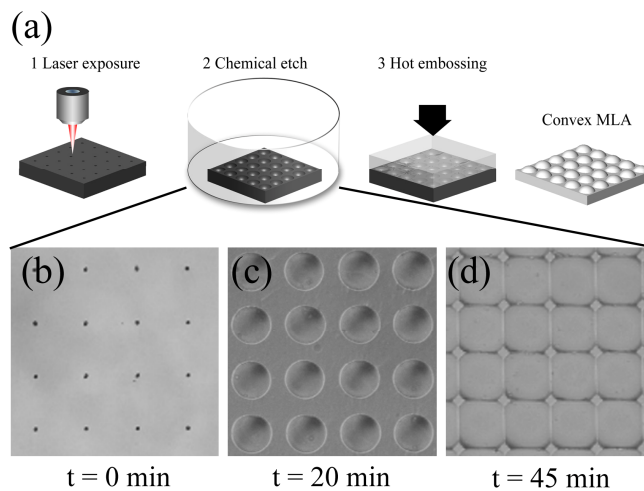


Figure 1. Fabrication process of the rectangular-shaped microlens array. (a) Schematic diagram of the procedures. (b) Optical microscope image of the ablation-induced crater array. (c) The circular concave surfaces are generated by the chemical etching for 20 minutes. (d) The circular patterns expand with the chemical etching process and contact with each other. The rectangular patterns are produced by 45-minutes chemical treatment.

For replication of convex structures, a self-made hot embossing system was used. The physical photograph of the system is given in Fig. 2. The PMMA sheet and mold were fixed onto upper and lower stages of the system. We heated the glass mold to  $120^\circ\text{C}$  by an electric heating template with a power of 400 W. The PMMA sheet was moved downwards and pressed on the heated mold for 5 minutes. The pressure was about 40 N which was measured by a pressure sensor mounted on the upper stage. Thereafter, the heating process was stopped and the temperature declined gradually. The stripping of PMMA sheet was made when the temperature below  $50^\circ\text{C}$ .

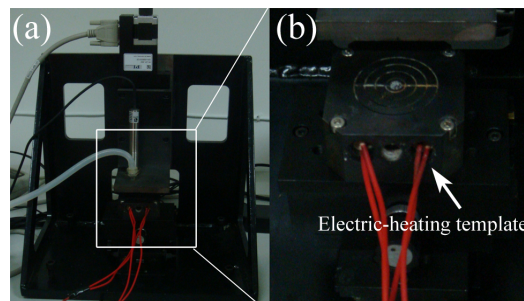


Figure 2. Hot embossing system. (a) The physical photograph of the hot embossing system. (b) The Electric-heating template.

The PMMA with convex structures on it was cleaned in ultrasonic path by DI water for 15 minutes. For SEM observations, the mold and PMMA sheet are both coated with Pt layers with thickness of about 10 nm. To obtain clear images of the 3D profiles of the microlenses, the samples for LCM investigations were covered with 25-nm Pt layers to increase the reflection of light.

### 3. RESULTS AND DISCUSSION

#### 3.1 Molding template

Figure 3 shows the morphology of the mold for fabrication of close-packed MLA. To measure the size of the microlenses, 3D profile of 100 concave surfaces was obtained by the LCM, and the result is shown in Fig. 3 (a). The insertion presents the cross-section profiles of the patterns, which are close to a spherical surface. The average width of the rectangular patterns is about  $60.4\text{ }\mu\text{m}$ , which equals to the interspacing of the laser-exposure spots. The sag height of the structures is about  $5.8\text{ }\mu\text{m}$ . We should note that the size of the structures dependent on the parameters used in the experiments. For example, the width is determined by the interspacing as mentioned in the section 2, and the sag height is closely related to the laser conditions such as the laser power, exposure time and the position of the focal plan. Generally, the deeper concave surfaces tend to be fabricated by a longer exposure time with a higher fluence. In addition, the uniformity of the structures is associated with the etching speed of the concave surfaces, which is sensitive to the laser conditions. In other words, an identical exposure time combined with a stable output of laser pulses plays a key role in manufacturing of uniform arrayed structures. In the experiment, multiple shots are commonly employed to minimize the impact of the slight fluctuation of the laser output. It is worth to mention that the alignment, shape and fill factors of the MLA can be flexibly tuned using these parameter-dependent regulations and accuracy control of the positions of the laser exposure spots and chemical etching time. Figs. 3 (b) and (c) show the SEM images of the mold, demonstrating that the uniform and smooth surfaces can be produced by this method.

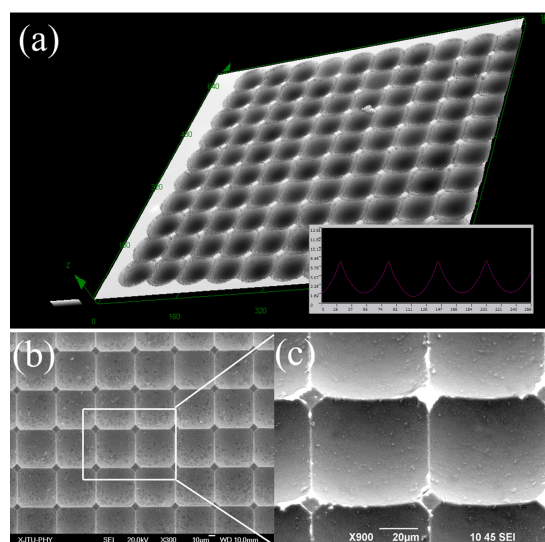


Figure 3. Morphology of the mold for fabrication of MLA. (a) 3D profile and cross-section profile of the structures. The results are obtained by a 3D laser confocal microscope. (b) SEM images of the mold (The visual angle,  $\theta = 90^\circ$ ). (c) Magnification of Fig. 3 (b) ( $\theta = 60^\circ$ ).

#### 3.2 Replication results

Figure 4 shows the result of the rectangular-shaped MLA replicated by the fabricated mold. Fig. 4 (a) shows the SEM result of the morphology of the MLA, visually expressing the comparable uniformity and smooth surface of the microlenses fabricated by this method. The LCM results are given in Figs. 4 (b) and (c). In Fig. 4 (c), we can see that the microlenses are packed very close and the gaps between them are not found. It is important for the application of microlenses because all the incoming lights will be focused through the lenses, which benefits for high-sensitive detections.

The LCM measurement shows that the width of the microlens is 59.9  $\mu\text{m}$ , which is 0.5  $\mu\text{m}$  smaller than the mold. The average height of the convex microlens is about 5.6  $\mu\text{m}$ , which is 0.2  $\mu\text{m}$  lower than the mold. The results of the mold and replica, which are obtained via the LCM investigations, and the deviations between the mold and replica, are listed in Tab. 1. The deviations of the width and height between the mold and replica are 0.83% and 3.5%. The results indicate that the structures can be faithfully replicated from the mold by this hot embossing process, demonstrating the excellent reproducibility of this method.

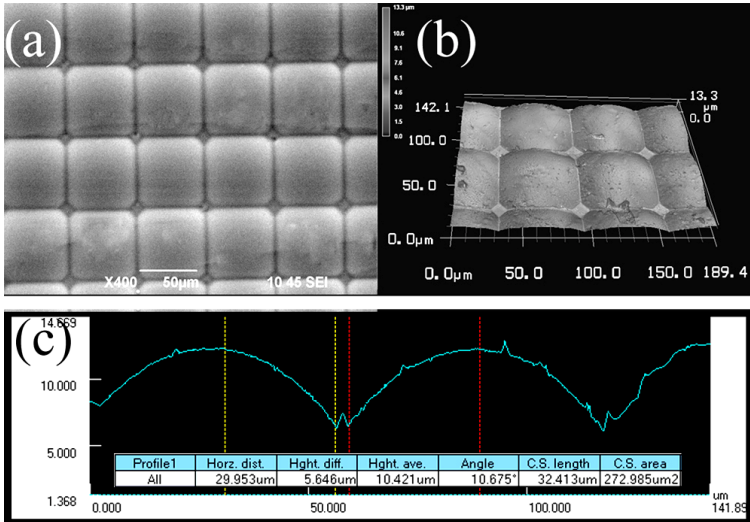


Figure 4. Replication of the MLA on PMMA. (a) SEM observation of the MLAs ( $\theta = 90^\circ$ ). (b) 3D profile of the MLA which is captured by a 3D laser confocal microscope. (c) Cross-sectional profile and the measured results of the MLAs. The average height of the microlenses is 5.646  $\mu\text{m}$ , and the width is 59.906  $\mu\text{m}$ .

Table 1. Sizes of the molding template and the replicas.

| Size ( $\mu\text{m}$ ) | Measurement Results |             |               |                   |
|------------------------|---------------------|-------------|---------------|-------------------|
|                        | Mold (M)            | Replica (R) | Deviation (D) | $\Delta$ (%)      |
| Width ( $r$ )          | 60.4                | 59.9        | 0.5           | 0.83 <sup>a</sup> |
| Height ( $h$ )         | 5.8                 | 5.6         | 0.2           | 3.5               |

### 3.3 Optical performances of the MLAs

The focal length of the MLA was measured by a system equipped with a He-Ne laser source (632 nm), a computer-controlled one-dimensional stage, an objective lens (NA = 0.15) and a CCD camera. The optical setup can be found in other literature<sup>10</sup>. The MLA is placed between the laser source and the lens; a clear image of the microlenses can be observed. By moving the MLA along the optical axis, the focal spots produced by the microlenses are captured by the CCD camera, and the distance is served as the focal length. The value is about 180  $\mu\text{m}$ . This result is similar to the calculated value obtained by the following equations:

$$P = (\eta^2 + \rho^2) / 2\eta,$$

$$\Phi = P / (\nu - 1)$$

Where  $\eta$  is the sag height of microlenses,  $\rho$  is the radius of the lenses,  $P$  is the curvature radius of the lenses,  $\phi$  is the focal length and  $\nu$  denotes for the refractive index of the PMMA. Considering  $\nu = 1.49$ , the calculated value of the focal length,  $\phi$ , is 169.7  $\mu\text{m}$ . The focal spots captured by the CCD camera and its density distribution image are shown in Figs. 5 (a) and (b), respectively. It implies an excellent light-gathering capability and comparable uniformity of the fabricated MLA.

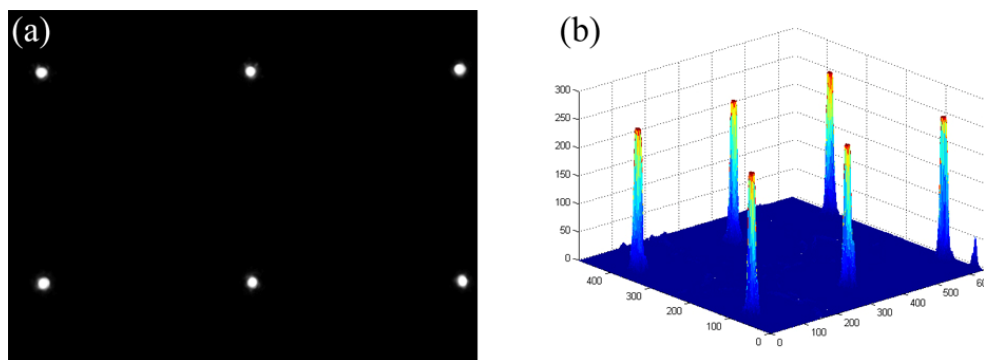


Figure 5. Focal spots of the MLA. (a) The microscope image of the focal spots captured by a CCD camera. (b) The density distribution of the focal spots shown in Fig. 5 (a).

To investigate the imaging properties of the microlenses, we used a microscope system with a CCD camera and a  $5\times$  objective lens (Nikon, NA=0.15). A transparent polymer film with typed letters “fs” was inserted between the light source (tungsten light) and the MLA, and the images were captured on the other side, as shown in Fig. 6. The images of letters are uniform and clear, which demonstrate the high qualities of the fabricated microlenses.

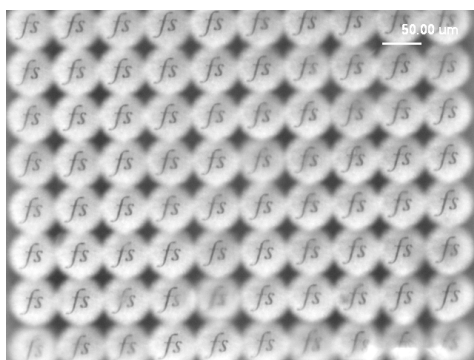


Figure 6. The images of the letters “fs” produced by the rectangular-shape microlens array.

### 3.4 Microlens arrays with different shapes

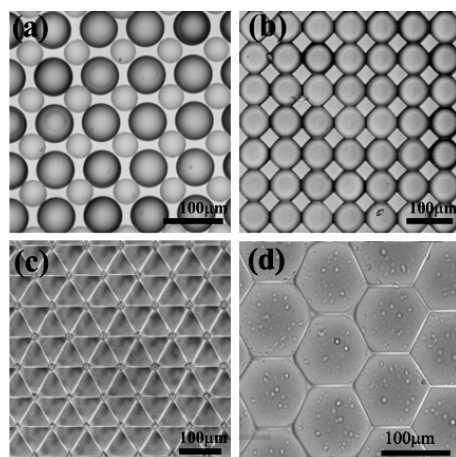


Figure 7. Microlens arrays with different shapes. (a) Circular-shape microlenses with two different sizes. (b) Diamond microlens arrays. (c) Triangle-shape microlens array. (d) Hexagonal-shape microlens array.

This method was used to fabricate various microlens arrays with different shapes, as shown in Fig. 7. The circular-shape microlens array with two different microlens sizes was obtained by additive embedding a rectangular-aligned microlens array into another one (Fig. 7 (a)). The control of the lens size via laser power was demonstrated in our previous work<sup>10</sup>.

The diamond, triangle and hexagonal-shape microlens arrays can be achieved by clever arrangement of laser exposure spots, which are demonstrated in Figs. 7 (b)-(d).

#### 4. SUMMARY

In summary, a closed-packed microlens array (MLA) with rectangular-shaped spherical microlenses is fabricated by a two-step process. First, a mold with concave structures was produced on a silica glass using a femtosecond-laser. By means of *in situ* laser-exposures, modified spots were created on sample surface point-by-point. When the laser-treated silica template was immersed in 5% hydrofluoric (HF) acid solution, concave spherical surfaces were self-formed in the modified spots. In the experiment, the rectangular patterns with a width of 60  $\mu\text{m}$  were fabricated by a 45-minutes chemical etching process. Second, the silica mold with concave structures was used to replication of plano-convex MLA on a Poly(methyl methacrylate) [PMMA] sheet with thickness of 1 mm using a self-made hot embossing system. The size of the MLA and mold were measured by an electronic scanning microscope and a laser confocal microscope. The comparison of the results between the mold and replica demonstrates the comparable reproducibility of this method. For optical properties, focal length of the MLA was measured; the result matches well with the calculated value. In addition, the ability to fabricate various MLAs with different shapes was also demonstrated in this work. This method provides an alternating approach for the fast fabrication of large-area polymeric microlenses and microlens arrays with various shapes.

#### REFERENCES

- [1] H. Yang, C. K. Chao, C. P. Lin, and S. C. Shen, "Micro-ball lens array modeling and fabrication using thermal reflow in two polymer layers," *J. Micromech. Microeng.*, vol. 14, pp. 277-282, 2004.
- [2] M. V. Kunnavaakkam, F. M. Houlihan, M. Schlax, J. A. Liddle, P. Kolodner, O. Nalamasu, and J. A. Rodgers, "Low-cost, low-loss microlens arrays fabricated by soft-lithography replication process," *Appl. Phys. Lett.*, vol. 82, pp. 1152-1154, 2003.
- [3] C. R. King, L. Y. Lin, and M. C. Wu, "Out-of-Plane Refractive Microlens Fabricated by Surface Micromachining," *IEEE Photon. Technol. Lett.*, vol. 8, pp. 1349-1351, 1996.
- [4] M. H. Wu, C. Park, G. M. Whitesides, "Fabrication of arrays of microlenses with controlled profiles using gray-scale microlens projection photolithography," *Langmuir*, vol. 18, pp. 9312-9318, 2002.
- [5] B. K. Lee, K. J. Cha and T. H. Kwona, "Fabrication of polymer micro nano-hybrid lens array by microstructured anodic aluminum oxide (AAO) mold," *Microelectron. Eng.*, vol. 86, pp. 857-860, June 2009.
- [6] R. Guo, S. Xiao, X. Zhai, J. Li, A. Xia and W. Huang, "Micro lens fabricated by means of femtosecond two photon photopolymerization," *Opt. Express*, vol. 14, pp. 810-816, January 2006.
- [7] J. Bonse and J. Krüger, "Probing the heat affected zone by chemical modifications in femtosecond pulse laser ablation of titanium nitride films in air," *J. Appl. Phys.*, vol. 107, pp. 054902 (1-5), March 2010.
- [8] J. Bonse, K.W. Brzezinkab and A.J. Meixner, "Modifying single-crystalline silicon by femtosecond laser pulses: an analysis by micro Raman spectroscopy, scanning laser microscopy and atomic force microscopy," *Appl. Surf. Sci.*, vol. 221, pp. 215-230, July 2003.
- [9] M. Budiman, E.M. Hsu, H.K. Haugen and G.A. Botton, "Cross-sectional study of femtosecond laser bulk modification of crystalline  $\alpha$ -quartz," *Appl. Phys. A: Materials Science & Processing*, vol. 98, pp. 849-853, January 2010.
- [10] F. Chen, H. Liu, Q. Yang, X. Wang, C. Hou, H. Bian, W. Liang, J. Si and X. Hou, "Maskless fabrication of concave microlens arrays on silica glasses by a femtosecond-laser-enhanced local wet etching method," *Opt. Express*, 18, 20334, 2010.